International Journal of Nanoelectronics and Materials
IJNeaM
ISSN 1985-5761 | E-ISSN 2232-1535

Numerical Simulation of Dielectrically Modulated Junctionless Accumulation mode FinFET for Biomolecule Detection

G. Durga Jayakumar [a] *, Abiisek M [a], Gayathri S [a], and Jesline N [a]

[a] *Sri Sivasubramaniya Nadar College of Engineering, Chennai, India-603110*
∗ Corresponding author. e-mail: durgag@ssn.edu.in

Received 30 May 2024, Revised 16 December 2024, Accepted 7 February 2025

ABSTRACT

This work investigates the detection of biomolecules using a junctionless accumulation mode Fin-type field-effect transistor (FinFET) as a dielectric modulated biosensor for medical diagnostics and food analysis applications. This study focuses on detecting neutral biomolecules, namely Keratin, Zein, Aminopropyltriethoxysilane (APTES), Biotin, and Streptavidin. Sentaurus technology design (TCAD) simulator is used in this work for the simulations. The variation in different electrical parameters of the device, namely switching ratio (I_{ON}/I_{OFF}), transconductance (g_m), and threshold voltage (V_{th}), is observed when neutral biomolecules are introduced inside the cavity with respect to their dielectric properties. The device's performance is analyzed by varying its parameters, including cavity thickness, cavity length, fin height/width, and doping concentration in the channel, as well as source/drain regions. The results are then compared with those of an under-gate dielectric modulated junctionless fin-type field-effect transistor having similar dimensions, and it is noticed that a significant improvement in biosensing is achieved by moving to a junctionless accumulation mode FinFET biosensor.

Keywords: *Biomolecules, Biosensor, JAMFET, Junctionless, Sensitivity, TCAD.*

1. INTRODUCTION

Biosensors are widely used in biomedical, food processing, and various other industries. Field-effect transistor (FET) biosensors are commonly utilized for biomolecule detection due to their compact size & weight, and potential for integration in a single chip [1]. FET biosensors can detect both charged and neutralized biomolecules. Neutralized biomolecules can be sensed in a dry condition, whereas the charged biomolecules can be detected in wet conditions. The dielectrically modulated FET biosensors receive more attention due to their potential to detect both charged and neutralized biomolecules [2-3].

The Metal-oxide-semiconductor FET (MOSFET), scaling down below 45 nm, would be fraught with numerous significant technological challenges, which include Short Channel Effects (SCEs), gate leakage through tunneling, and Drain Induced Barrier Lowering (DIBL) that restricts the scaling of a single gate planar CMOS transistor [4-5]. In comparison to traditional planar single-gate MOSFET and double-gate MOSFET, the non-planar FinFET exhibits a high I_{ON}/I_{OFF} ratio, decreased subthreshold swing, and tolerance to short channel effects because of its improved gate controllability [6-7]. One of the solutions to the scaling problem is junctionless FET [8]. Junctionless (JL) transistors offer several advantages, including the absence of n-p junctions, a single dopant (either n+ or p+) at the same doping level in the source, drain, and channel, a simple fabrication process, reduced variability, and improved SCE and DIBL performance [9-10]. Since there is no junction between the source/drain and the channel, a junctionless device does not require steep doping profiles. To achieve this, a higher doping concentration is needed. Still, it also results in poor carrier mobility, threshold voltage (V_{th}) variation, and a requirement for a high metal gate work function [11-12]. It is suggested that the channel doping concentration must be low to achieve an appropriate threshold voltage (V_{th}), a low sub-threshold swing (SS), and a high I_{ON}/I_{OFF} ratio [13], resulting in a junctionless accumulation mode (JAM) FET. The JAM device is similar to the junctionless device in design, but its doping concentration varies between the source/drain region and the channel, which is beneficial over the existing conventional junctionless devices in terms of improved mobility, better I_{ON}/I_{OFF} ratio, improved SS, reduced parasitic resistance, and DIBL effect [14-15].

Different FET structures have been analyzed as a biosensor in the literature. A lot of work has been done on Tunnel FETs [16-17]. A double-gate MOSFET structure is studied for its biosensing applications in the literature [18]. Junctionless dielectric modulated FET structures are actively analyzed in various literature. Dielectric modulated GaAs junctionless FinFET as a biological sensor in the sub-20 regimes is discussed in [19]. The symmetrical design of a double gate dielectric modulated junctionless tunnel FET structure is investigated in [20] as a biosensor. The bulk planar junctionless FinFET is analyzed as a biosensor in the presence of noise [21]. An analytical model of a trench dual gate junctionless FET biosensor is described in [22]. A dielectric modulated split-gate junctionless bio-FET to detect the analytes has been investigated, and its analytical model has also been developed [23]. An analytical model for

a junctionless FinFET biosensor is developed, and a comparison is also made with a junctionless nanowire FET [24]. In the literature, the recent nanostructures [25], namely nanowires and nanotubes, are also being explored for biosensing applications. Beyond this, FET-based biosensors have also been used for the detection of nucleic acids [26]. The recent advancements in materials help to improve the features of biosensors using graphene-based carbon nanotubes [27]. However, no attempts have been made to use the JAM FinFET as a biosensor device.

1.1. Contribution

Although the device performance of JAM FinFET has been explored in the literature, its bio-sensing performance remains uninvestigated. The novelty of this work is to investigate the possibility of using the JAM FinFET as a biosensor under a dielectrically modulated approach. This paper presents the JAM FinFET biosensor and analyzes its performance based on 3D technology computer-aided design (TCAD) simulations.

(i) In this work, the proposed JAM FinFET biosensor is designed as an Under-gate Dielectric Modulated (UGDM) biosensor to detect neutral biomolecules. It is placed in the cavity, which has a unity dielectric constant, which is air. The biomolecules are placed in the device's nanogap cavity [28-29], which has a different dielectric constant (K) for each biomolecule (Streptavidin: 2.1, biotin: 2.63, APTES: 3.57, Zein: 5, and Keratin: 8) [30]. This difference enables the device to detect the biomolecules using the principle of the dielectric modulation approach. Upon introducing those neutral biomolecules inside the nanogap cavity under the gate, there is a change in gate oxide capacitance, which alters the electrical characteristics, namely threshold voltage, drive (I_{ON}) current, leakage (I_{OFF}) current, and transconductance of the device. The change in electrical characteristics helps in detecting particular biomolecules.

(ii) The optimization of the UGDM JAM FinFET biosensor is also carried out by varying the cavity length (Lc), thickness of the cavity (Tc), and also varying the doping concentration of the channel (Nch), as well as source (Ns) and drain (Nd) to improve the I_{ON}/I_{OFF} ratio sensitivity.

(iii) The optimized UGDM JAM FinFET biosensor is compared with the Junctionless FinFET (UGDM JL FinFET) biosensor for its sensitivity. It concludes that the UGDM JAM FinFET biosensor shows significant improvement in I_{ON}/I_{OFF} ratio and threshold voltage sensitivity than the UGDM JL FinFET biosensor. Further, the threshold voltage sensitivity of the UGDM JAM FinFET biosensor is analyzed for variation in cavity thickness, fin height/width, and cavity filling capacity. With the help of Sentaurus TCAD [31], the device design, simulation, and analysis are carried out at ease.

2. STRUCTURE OF UGDM JAM FINFET

The proposed device structure in this work, the Under-gate Dielectric Modulated Junctionless Accumulation Mode FinFET (UGDM JAM FinFET) based biosensor, is represented with dimensions in Fig. 1(a), and the conventional structure of UGDM JL FinFET is shown in Fig. 1(b). The fin structure comprises the source, drain, and channel structure that is formed on top of the SOI substrate. The JAM FinFET uses a gate structure that can accumulate electrons in the channel region, creating a conductive path between source and drain. The source and drain have a higher doping level than the channel and do not have any junctions, which lead to better performance of the device. The detailed specifications [9], including dimensions and doping concentration of the devices UGDM JL FinFET and UGDM JAM FinFET, are given in Table 1. A small nanocavity is desirable for improving the sensitivity of the FET-based biosensors. Hence, the thickness of the cavity used for biosensing is developed with reference to the literature [28]. As the cavity is under the gate, its length is the same as that of the gate length (20nm). All the parameters are the same for both Junctionless FET and JAM FET, except the doping concentration. The following models are used for all simulations of the results: the Field-dependent mobility model, the doping-dependent mobility model, and the Lombardi mobility model, which is appropriate for non-planar structures. Drift–diffusion model and the Fermi-Dirac model are also used for carrier transport. In addition to these, SRH models are utilized for the recombination and generation of charge carriers. Apart from these, a Band2Band model is also incorporated for the carriers tunneling between the valence band and conduction band.

The sensing of biomolecules is done using the nanogap cavity that is formed below the gate contact, which is filled with the biomolecules. Biomolecules having different dielectric constants are not mobilized in the cavity, which changes the gate capacitance of the device. This leads to a change in the electrical behavior of the device, such as the ON current and threshold voltage. The neutral biomolecules having K > 1 and between 2 and 8 have been chosen [30] to observe the effect of biomolecules on the characteristics of the proposed UGDM JAM FinFET biosensor and are as follows: Streptavidin with K-2.1, Biotin with K-2.63, APTES with K-3.57, Zein with K-5, and Keratin with K-8. These five biomolecules have been chosen because of their usefulness as follows; Streptavidin is mainly used for detection of protein; Biotin helps to control blood sugar level and hair fall; APTES (3-aminopropyl triethoxysilane) is primarily used for the handling of acidic oil; Zein is a prolamine protein which is useful for drug-delivery in food applications; and Keratin is a protein largely helpful for making hormones and repairing tissues [32].

Table 1. Device Description.

Device Parameters	UGDM JAM FinFET biosensor	UGDM JL FinFET biosensor
Substrate (nm)	60 × 20 × 20	60 × 20 × 20
Channel	40 × 8 × 12 nm	40 × 8 × 12 nm
fin height	12 nm	12 nm
fin width	8 nm	8 nm
Source/ Drain (nm)	10 × 8 × 12	10 × 8 × 12
Cavity length (Lc)	20 nm	20 nm
Cavity thickness (Tc)	1.5 nm	1.5 nm

Source/Drain doping (Nsd)	1×10^{19} cm^{-3}	1×10^{18} cm^{-3}
Channel doping (Nch)	1×10^{18} cm^{-3}	1×10^{18} cm^{-3}

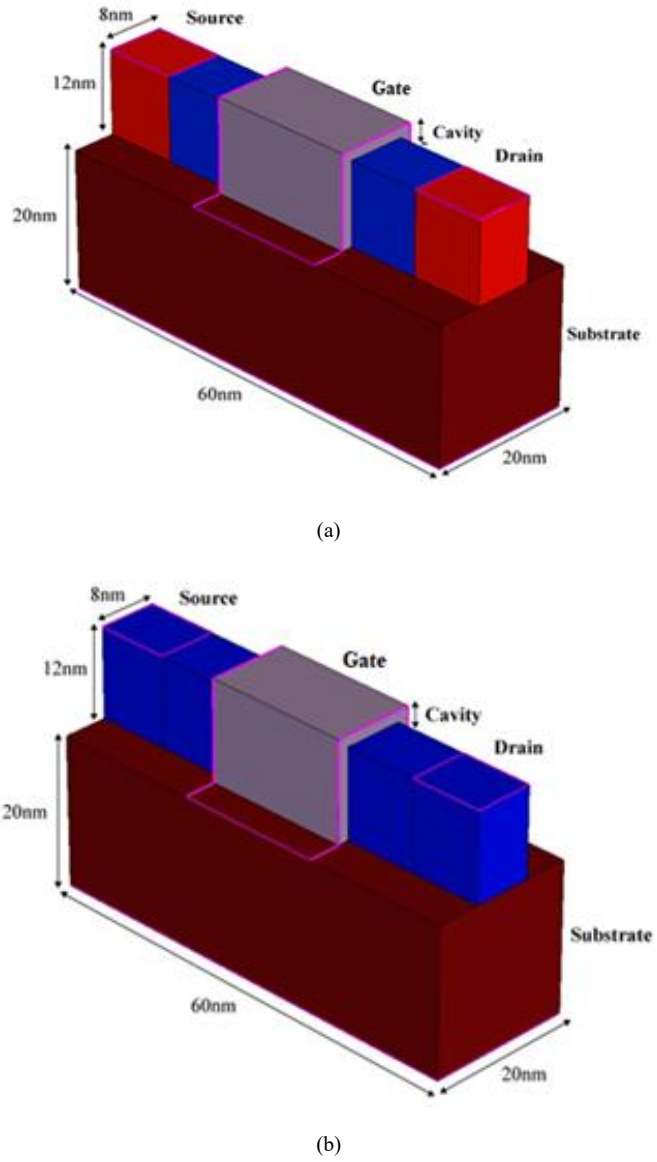

Figure 1. Device structure with dimensions (a) proposed UGDM JAM FinFET biosensor (b) UGDM JL FinFET biosensor.

2.1. Calibration of UGDM JAM FinFET biosensor

The JAM FinFET biosensor has been simulated and calibrated for its $I_D - V_{GS}$ characteristics. Figure 2 represents the calibration curve of drain current (I_D) vs gate voltage (V_{GS}) for various biomolecules. The graph plots drain current for drain voltage V_{DS} at 0.3 V. Upon introducing the neutral biomolecules with K > 1 inside the nanogap cavity, significant variations were observed in the output current characteristics, I_{ON}/I_{OFF} ratio, transconductance, and threshold voltage (V_{th}). Here, the nanogap cavity region serves as a sensing region, and the biomolecules are immobilized there. If there are no biomolecules in the nanogap cavity region, then the air (K = 1) will be filled in that cavity. The I_{ON}/I_{OFF} ratio is a key parameter that determines the sensitivity of a biosensor for the given device, as it depends on both I_{ON} and I_{OFF}. I_{ON} is measured when V_{GS} = 1 V, and I_{OFF} is measured when V_{GS} = 0 V. As shown in Figure 2, I_{OFF} decreases as the K value increases, with only minor changes in I_{ON}, increasing the I_{ON}/I_{OFF} switching ratio. This is because of enhanced gate control over the channel. Figure 3 represents the comparison of the I_{ON}/I_{OFF} ratio of the UGDM JAM FinFET biosensor with the UGDM JL FinFET biosensor for various biomolecules placed in the cavity. It says that the I_{ON}/I_{OFF} ratio increases as the K value increases for both devices. This is due to the respective increase in the electric field [28]. However, the improvement in the I_{ON}/I_{OFF} ratio is more pronounced in the UGDM JAM FinFET biosensor compared to the UGDM JL FinFET biosensor because the UGDM JAM FinFET biosensor has a higher drain current than the JL FinFET biosensor, and this is due to the higher mobility of charges in the channel [14].

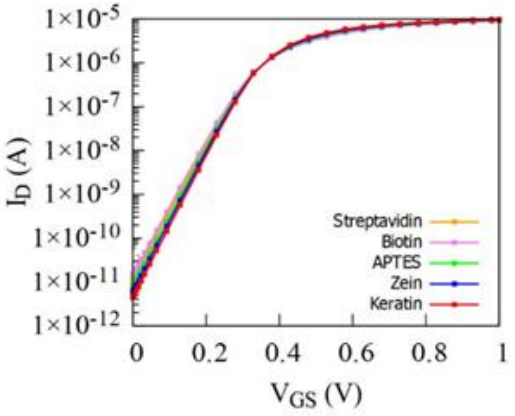

Figure 2. $I_D - V_{GS}$ Characteristics of UGDM JAM FinFET biosensor for various biomolecules.

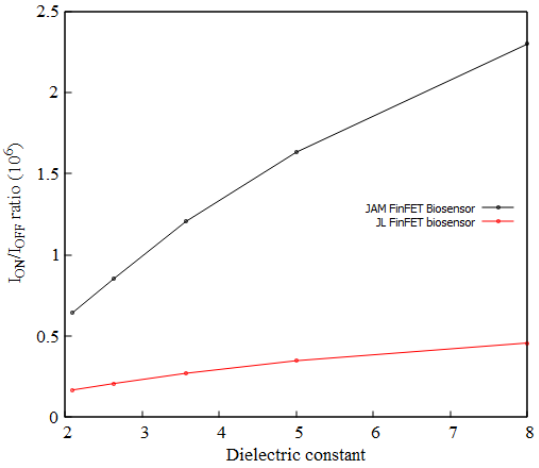

Figure 3. I_{ON}/I_{OFF} ratio comparison of UGDM JAM FinFET biosensor with UGDM JL FinFET biosensor for various biomolecules.

Figure 4 depicts the variation in energy bands of the UGDM JAM FinFET under the ON state when neutral biological molecules having various dielectric constants are present in the cavity. Here, it is seen that the band bending at the source to channel junction is due to the immobilization of dielectric biomolecules inside the cavity. It is also observed that as the K value increases, more band bending occurs at the junction, resulting in a decrease in the tunneling barrier

height of the source to channel junction. This aspect enriches the source to channel coupling [30]. Figure 4 illustrates a larger barrier for air and a smaller barrier for the Keratin biomolecule, which has the highest K of 8 among the five biomolecules.

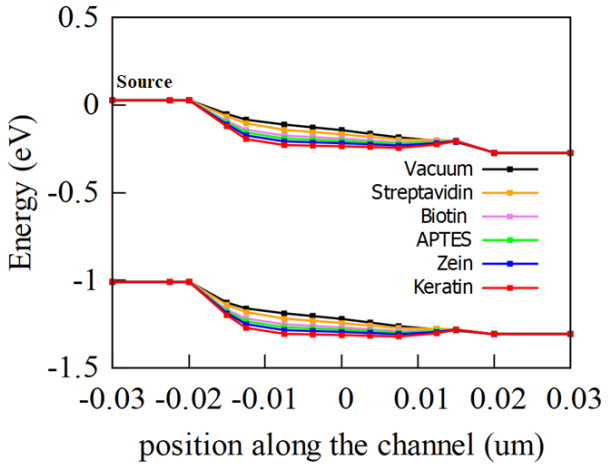

Figure 4. Energy band profile along the channel of the device UGDM JAM FinFET biosensor.

3. OPTIMIZATION OF UGDM JAM FINFET BIOSENSOR

The designed and calibrated UGDM JAM FinFET biosensor device is set to be optimized against process variation. The parameters chosen for optimization are (i) the length of the cavity (Lc), (ii) the thickness of the cavity (Tc), and (iii) the doping concentration of the regions: channel (Nch) and source/drain (Nsd). These parameters are varied for all the biomolecules of different dielectric constants (K = 2 to 8). Using the process variation analysis, the impact of the above-mentioned parameters on the I_{ON}/I_{OFF} ratio is studied. This study is helpful to obtain an optimized UGDM JAM FinFET biosensor device for its sensitivity.

3.1. The Cavity length (L_C)

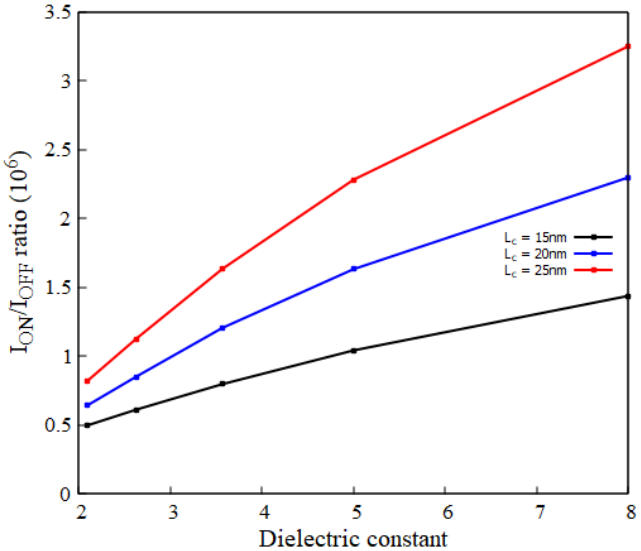

Figure 5. Dielectric constant vs I_{ON}/I_{OFF} ratio for various Cavity lengths (Lc) of UGDM JAM FinFET biosensor.

The device depicted in Figure 1(b) has the gate contact above the cavity region, and the length is 20nm. Taking into account the area of contact for the biomolecules to act on and the physical constraints on the device, the cavity length is varied from 15nm to 25nm for a constant K. As seen from Figure 5, the I_{ON}/I_{OFF} ratio is at the maximum when the cavity length is extended to 25nm. The widespread contact of biomolecules with the channel region leads to an increase in the motion of free charge carriers from valence to conduction band, which accounts for the increased switching (I_{ON}/I_{OFF}) ratio [21]. This result applies to all the biomolecules used.

3.2. The Cavity Thickness (T_C)

The cavity between the channel and the gate is the area where all the biomolecules are injected, which in turn changes the dielectric constant under the gate and changes the device characteristics. Figure 6 illustrates that, for a constant K, decreasing the cavity thickness causes the I_{ON}/I_{OFF} ratio to increase slowly, due to the increased gate contact with the channel. Gate oxide capacitance is inversely proportional to the distance between the conducting plates, and the biomolecules act as an insulator between the gate and the channel [21]. Hence, from Figure 6, the plot with a cavity of thickness 1nm gives the highest current ratio compared to those with 1.5 nm and 2 nm thicknesses. This pattern applies to all the biomolecules (K > 1) used.

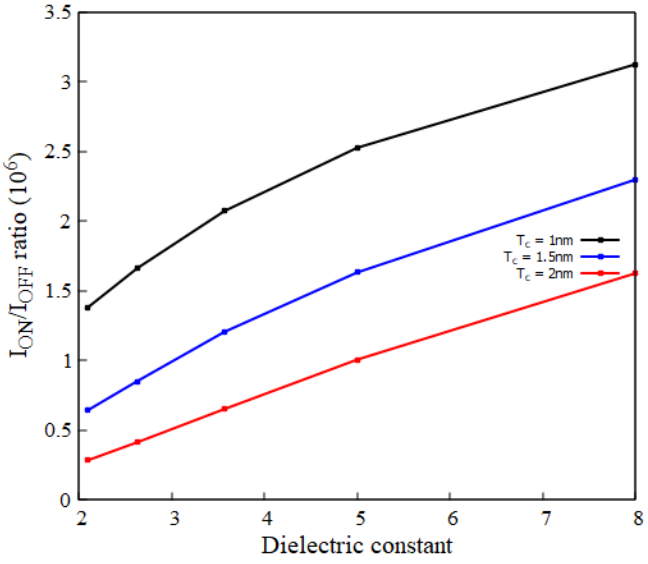

Figure 6. Dielectric constant vs I_{ON}/I_{OFF} ratio for various Cavity thickness (Tc) of UGDM JAM FinFET biosensor.

3.3. Variation in doping concentration

The various device regions, source, drain, and channel, have doping concentrations as mentioned in Table 1. To yield better results for the ease of biomolecule detection, the doping profiles are varied. Figure 7 shows the variation of the I_{ON}/I_{OFF} ratio of UGDM JAM FinFET biosensor for various combinations of doping concentration in source (S), channel (C), and drain regions (D). In JAM FinFET, reducing the doping concentration in the channel leads to a reduction in the parasitic resistance. From Figure 7, the doping combinations (i) S = 1e19cm^{-3}, C=1e17cm^{-3}, D=1e19cm^{-3}

and (ii) S = 1e19cm^{-3}, C = 1e17cm^{-3}, D = 1e18cm^{-3} provide the highest I_{ON}/I_{OFF} ratio than other possible combinations. Next, the set of the following three doping combinations, (i) S = 1e19cm^{-3}, C = 1e18cm^{-3}, D = 1e19cm^{-3}, (ii) S = 1e19cm^{-3}, C = 1e18cm^{-3}, D = 1e18cm^{-3} and (iii) S = 1e19cm^{-3}, C = 1e18cm^{-3}, D = 1e17cm^{-3} provides the better I_{ON}/I_{OFF} ratio with reference to variation in drain doping. The doping combination of S = 1e17cm^{-3}, C = 1e18cm-3, D = 1e19cm^{-3} provides the least I_{ON}/I_{OFF} ratio because of the reduction of doping concentration in the source region. Hence, the proposed UGDM JAM FinFET biosensor with doping of S = 1e19cm^{-3}, C = 1e18cm^{-3}, D = 1e19cm^{-3} is optimally chosen for further analysis.

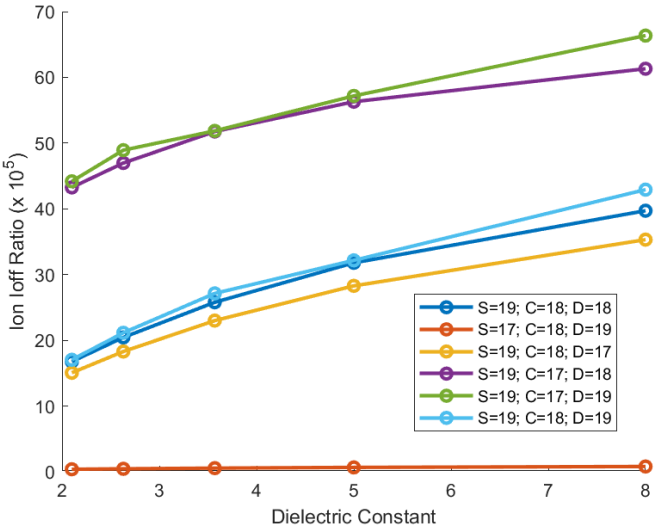

Figure 7. Dielectric constant vs I_{ON}/I_{OFF} for varying doping concentrations in the source (S), channel (C), and drain regions (D) of a UGDM JAM FinFET biosensor.

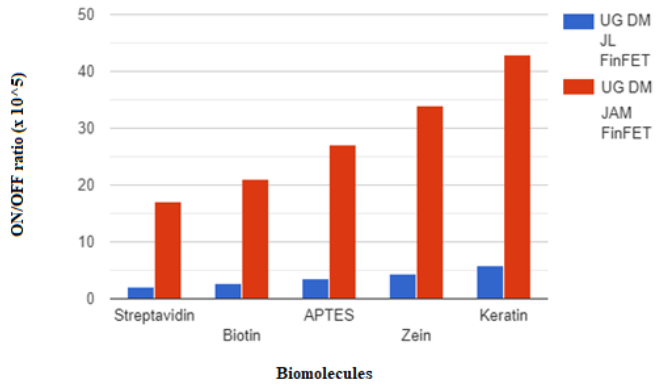

Figure 8. Comparison of the I_{ON}/I_{OFF} ratio of UGDM JAM FinFET and UGDM JL FinFET with optimized values of cavity length Lc = 25nm and cavity thickness Tc = 1nm.

From Figures 5 and 6, an increase in cavity length and a decrease in cavity thickness can lead to an improved I_{ON}/I_{OFF} ratio. Hence, the cavity length Lc = 25nm and cavity thickness Tc = 1nm are chosen as the optimized values for further study. Figure 8 shows the comparison of the I_{ON}/I_{OFF} ratio results of the proposed UGDM JAM FinFET with UGDM JL FinFET for different biomolecules. As shown in Figure 8, the I_{ON}/I_{OFF} ratio increases significantly with the K value for the proposed UGDM JAM FinFET compared to UGDM JL FinFET. This is due to increased mobility in JAMFET, which results in an increase in ON current with reduced OFF current and thereby a higher I_{ON}/I_{OFF} switching ratio.

4. SENSITIVITY ANALYSIS OF OPTIMIZED UGDM JAM FINFET BIOSENSOR

To study the sensitivity performance, threshold voltage (V_{th}), threshold voltage sensitivity (S_{Vth}), and transconductance of the optimized UGDM JAM FinFET are considered.

4.1. UGDM JAM FinFET threshold Voltage (V_{th}) and threshold voltage sensitivity (S_{Vth})

The threshold voltage is considered one of the sensing parameters that detects the interaction of biomolecules with the sensing area of the UGDM JAM FinFET biosensor. The variation of threshold voltage (V_{th}) and threshold voltage sensitivity (S_{Vth}) for neutral biomolecules with different dielectric constants (K) is shown in Figures 9 and 10, respectively. The V_{th} is obtained from the DC transfer characteristics, and the S_{Vth} is calculated by the difference in the value of the threshold voltage with and without the biomolecules as ($S_{Vth} = V_{th}(K > 1) - V_{th}(K = 1)$) [24].

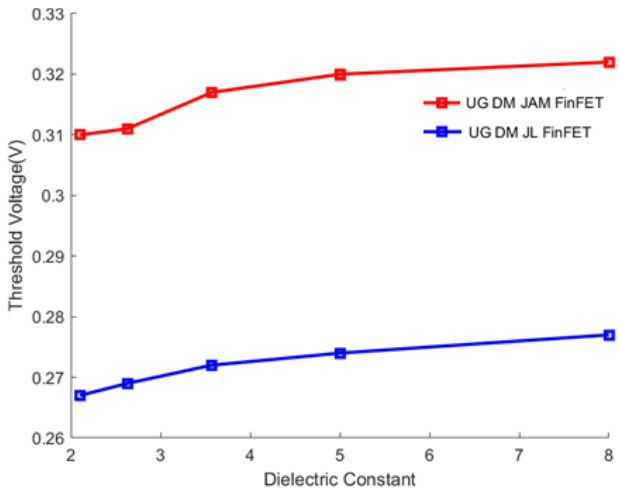

Figure 9. Threshold voltage variation (V_{th}) of optimized UGDM JAM FinFET and JL FinFET biosensors with the device dimensions Tc = 1 nm and Lc = 25 nm. Here, doping for UGDM JAM FinFET: S&D = 10^{19} atoms/cm^3; C=10^{18} atoms/cm^3 and for JL FinFET: S, D, C = 10^{18} atoms/cm^3

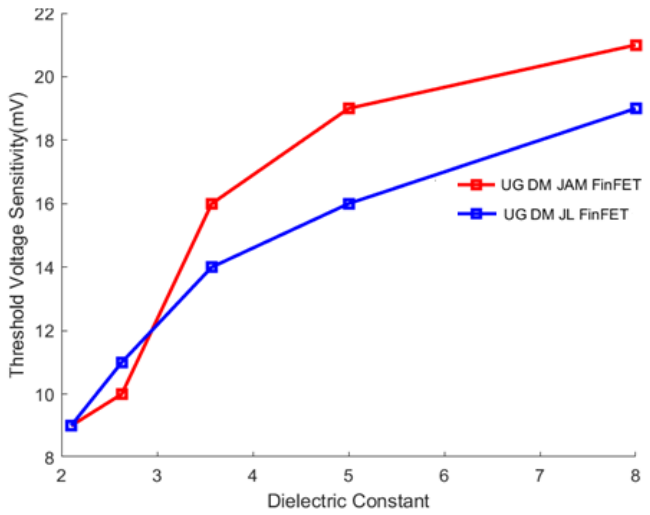

Figure 10. Threshold voltage sensitivity variation (S_{Vth}) of optimized UGDM JAM FinFET and JL FinFET biosensors with the device dimensions Tc = 1 nm and Lc = 25 nm. Here, doping for UGDM JAM FinFET: S&D = 10^{19} atoms/cm^3; C=10^{18} atoms/cm^3 and for JL FinFET: S, D, C = 10^{18} atoms/cm^3

From Figures 9 and 10, it is evident that the threshold voltage and threshold voltage sensitivity of the JAM FinFET biosensor increase upon the introduction of biomolecules with higher K values. As the permittivity increases, a higher gate voltage is needed for channel depletion and thus to turn the device OFF. UGDM JAM FinFET biosensor also shows a significant variation in V_{th} for different K values as compared to the JL FinFET. It therefore provides higher sensitivity for the detection of biomolecules. It is due to the additional source/drain implantation compared to the channel, which reduces high parasitic resistances and thereby increases conductivity.

4.2. Impact of Fin Height (H_{Fin}) and Fin Width (W_{Fin}) on threshold voltage sensitivity (S_{Vth})

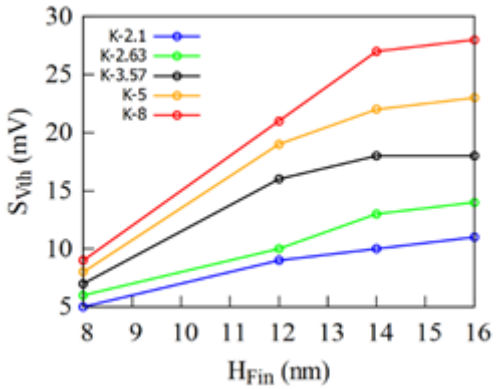

(a)

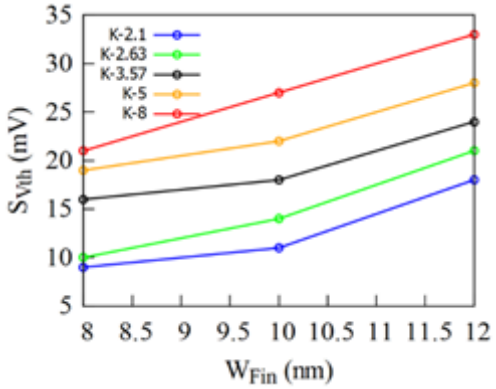

(b)

Figure 11. (a) fin height vs S_{Vth} (b) fin width vs S_{Vth} for different biomolecules of UGDM JAM FinFET

For various H_{Fin} and W_{Fin}, the S_{Vth} sensitivity has also been measured, and they are depicted in Figure 11. From Figure 11(a), it is observed that the S_{Vth} increases as the fin height increases for various biomolecules. This is because of the increased quantity of immobile biomolecules in the cavity [12,24]. It is also expected that the biomolecule streptavidin has the lowest S_{Vth} for all the fin heights. Figure 11(b) shows the same trend for fin width variation.

4.3. Impact of filling volume of cavity on threshold voltage sensitivity (S_{Vth})

It is expected that the cavity is uniformly filled with biomolecules. But in some bio-tests, there are some vacant spaces in the cavity. It means the cavity is partially filled with biomolecules. To capture this, the presence of biomolecules in the cavity is varied for 20%, 50% and 100%. Figure 12 shows the chart of S_{Vth} for the cavity filling of 20%, 50%, and 100% for different biomolecules. It shows the highest sensitivity for 100% filling of biomolecules in the cavity, and below that, the sensitivity is gradually reduced [20]. The least sensitivity is obtained for 20% filling. The same trend is followed for all the biomolecules. In addition to the filling volume, the location of biomolecules also decides the sensitivity. Figure 12 corresponds to the presence of biomolecules from one side of the fin towards the other side. It means the equal presence of biomolecules from the source side towards the drain side for the given cavity filling volume. For example, in 50% filling volume, one half of the source side, which supports the tunneling process at the source-channel junction, is filled with biomolecules, and the remaining half is filled with air.

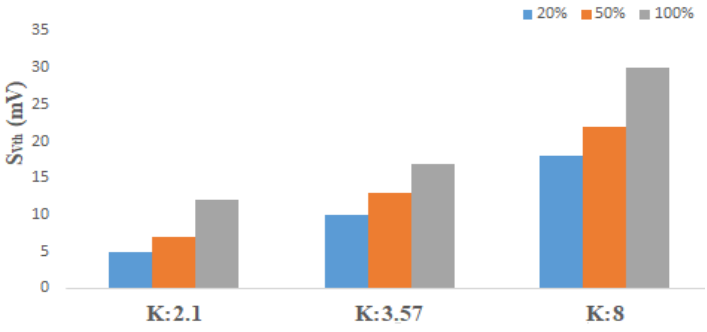

Figure 12. Change in S_{Vth} for three different cavity filling volumes of UGDM JAM FinFET.

4.4. Transconductance (g_m)

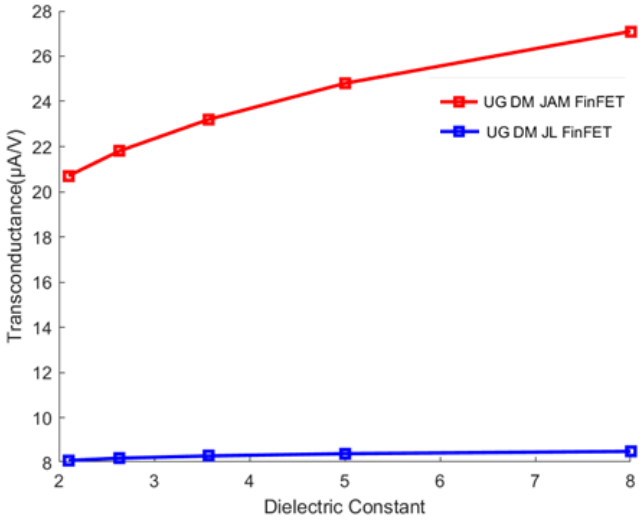

Figure 13. Transconductance variation for different biomolecules present in JAM FinFET and JL FinFET biosensors with the device dimensions Tc = 1 nm and Lc = 25 nm, Doping: UGDM JAM FinFET (S&D=10^{19} atoms/cm^3; C=10^{18} atoms/cm^3) and for JL FinFET (S, D, C=10^{18} atoms/cm^3)

The variation of the transconductance (g_m) for different biomolecules at V_{DS} of 0.3 V is shown in Figure 13. The change in V_{th} with the presence of biomolecules results in a shift in transconductance (g_m). As the K value increases, the transconductance also changes significantly for UGDM JAM FinFET than JL FinFET. Since g_m is directly related to the drain current, it increases with drain current (I_{ON}) for all the biomolecules used [24].

5. CONCLUSION

This research work proposed a JAM FinFET-based biosensor. A comparative study based on simulation is done for the UGDM JAM FinFET biosensor with the UGDM JL FinFET biosensor. The Sentaurus TCAD simulator is used to test the performance of the device.

To assess the sensitivity of the proposed JAM FinFET biosensor, various electrical parameters have been analyzed, including the drain current, I_{ON}/I_{OFF} ratio, threshold voltage, threshold voltage sensitivity, and transconductance. This study involved the optimization of the device performance by varying the cavity thickness, cavity length, and doping concentration in the source, drain, and channel regions. The results proved that increasing the cavity length and decreasing the cavity thickness could lead to improved I_{ON}/I_{OFF} ratio sensitivity. From the comparison results, it was found that the JAM FinFET performs better as a biosensor than the UGDM JL FinFET due to less mobility deterioration than the JL FinFET. Overall, the findings of this study suggest that the UGDM Junctionless accumulation mode FinFET is a promising candidate as a biosensor for detecting biomolecules in various applications. Furthermore, the device can be studied for sensitivity analysis of charged biomolecules and its sensitivity improvement by utilizing different source materials.

REFERENCES

[1] H. Im, X.-J. Huang, B. Gu and Y.-K. Choi, "A dielectric-modulated field-effect transistor for biosensing", *Nature Nanotechnol*., vol. 2, pp.430–434, 2007.

[2] C.-H. Kim, C. Jung, K.-B. Lee, H. G. Park and Y.-K. Choi, "Label-free DNA detection with a nanogap embedded complementary metal oxide semiconductor," *Nanotechnology*, vol. 22, 135502, 2011.

[3] M. Im, J.-H. Ahn, J.-W. Han, T. J. Park, S. Y. Lee and Y.-K. Choi, "Development of a point-of-care testing platform with a nanogap embedded separated double-gate field effect transistor array and its readout system for detection of avian influenza," *IEEE Sensors J*, vol. 11, pp. 351-360, 2011.

[4] Colinge, J.P, "FinFETs and Other Multigate Transistors" (Springer Berlin), 2007.

[5] Ferain, I., Colinge, C.A., and Colinge, J.P, "Multigate transistors as the future of classical metal-oxide-semiconductor field-effect transistors," *Nature*, vol. 479, pp.310-316, 2011.

[6] Hisamoto, D., et al, "FinFET-A self-aligned double-gate MOSFET scalable to 20 nm," *IEEE Trans. Electron Devices*, vol. 47, pp.2320-2325, 2000.

[7] D. Bhattacharya and N. K. Jha, "FinFETs: From devices to architectures" *Adv. Electron*., 365689, 2014.

[8] Gundapaneni, S., Ganguly, S. and Kottantharayil, A, "Enhanced electrostatic integrity of short channel junctionless transistor with high-k spacers," *IEEE Electron. Device Lett*., vol. 32, pp.1325-1327, 2011.

[9] Lee, C.-W., Afzalian, A., Akhavan, N.D., Yan, R., Ferain, I. and Colinge, J.P, "Junctionless multigate field-effect transistor," *Appl. Phys. Lett.,* vol. 94, pp.053511-1, 2009.

[10] Colinge, J.P., Lee, C.-W., Afzalian, A., Akhavan, N.D., Yan, R., Ferain, I., Razavi, P., O'Neill, B.,Blake, A., White, M., Kelleher, A.-M., McCarthy, B. and Murphy, R, "Nanowire transistors without junctions," *Nat. NanoTechnol.,* vol. 5, pp.225-229, 2010.

[11] T. K. Kim et al., "First Demonstration of Junctionless Accumulation-Mode Bulk FinFETs with Robust Junction Isolation," *IEEE Electron Device Letters*, vol. 34, pp.1479-1481, 2013.

[12] J. H. Choi, T. K. Kim, J. M. Moon, Y. G. Yoon, B. W. Hwang, D. H. Kim and S.-H. Lee, "Origin of device performance enhancement of junctionless accumulation-mode bulk FinFETs with high-k gate spacers," *IEEE Electron Device Letters*, vol. 35, pp.1182-1184, 2014.

[13] A. Dubey, R. Narang, M. Saxena and M. Gupta, "Investigation of single event transient effects in junctionless accumulation mode MOSFET," *IEEE Transactions on Device and Materials Reliability*, vol. 20, pp.604-608, 2020.

[14] Kumar, Bhavya and Rishu Chaujar, "Analog and RF performance evaluation of junctionless accumulation

mode (JAM) gate stack gate all around (GS-GAA) FinFET", *Silicon*, vol. 13, pp.919-927, 2021.

[15] Yadav,S., Rewari, S. and Pandey, R, "Junctionless Accumulation Mode Ferroelectric FET (JAM-FE-FET) for High Frequency Digital and Analog Applications," *Silicon,* vol. 14, pp.7245-7255, 2022.

[16] G. Wadhwa and B. Raj, "Label free detection of biomolecules using charge-plasma-based gate underlap dielectric modulated junctionless TFET", *J. Electron. Mater*., vol. 47, pp.4683-4693, 2018.

[17] Prabin Kumar Bera, Rashmi Rekha Sahoo, RajibKar and Durbadal Mandal, "Design and Sensitivity Investigation of Dielectric Modulated and Electrolyte-Based pH Sensing of Vertical TFET Biosensor," *IEEE T. on Nanotechnology,* vol. 22, pp.537-544, 2023.

[18] B. Buvaneswari and N. B. Balamurugan, "2D analytical modeling and simulation of dual material DG MOSFET for biosensing application", *AEU-Int. J. Electron. Commun.,* vol. 99, pp.193-200, 2019.

[19] A. Chhabra, A. Kumar and R. Chaujar, "Sub-20 nm GaAs junctionless FinFET for biosensing application," *Vacuum,* vol. 160, pp.467-471, 2019.

[20] G. Wadhwa and B. Raj, "Design, simulation and performance analysis of JLTFET biosensor for high sensitivity", *IEEE Transactions on Nanotechnology,* vol. 18, pp.567-574, 2019.

[21] D. Singh and G. C. Patil, "Dielectric-modulated bulk-planar junctionless field-effect transistor for biosensing applications", *IEEE Trans. Electron Devices,* vol. 68, pp.3545-3551, 2021.

[22] U. Soma, "A dual gate junctionless FinFET for biosensing applications," *Silicon,* vol. 14, pp.8881-8885, 2022.

[23] Ajay, R. Narang, M. Saxena and M. Gupta, "Modeling and Simulation Investigation of Sensitivity of Symmetric Split Gate Junctionless FET for Biosensing Application", *IEEE Sensors Journal,* vol. 17, pp.4853-4861, 2017.

[24] H. D. Sehgal, Y. Pratap, M. Gupta and S. Kabra, "Performance analysis and optimization of under-gate dielectric modulated junctionless FinFET biosensor", *IEEE Sensors Journal,* vol. 21, pp.18897-18904, 2021.

[25] S. Tayal, B. Majumdar, S. Bhattacharya and S. Kanungo, "Performance Analysis of the Dielectrically Modulated Junction-Less Nanotube Field Effect Transistor for Biomolecule Detection", *IEEE Transactions on NanoBioscience,* vol. 22, pp.174-181, 2023.

[26] C.-H. Kim, C. Jung, H. G. Park and Y.-K. Choi, "Novel dielectric modulated field-effect transistor for label-free DNA detection", *Biochip J*., vol. 2, pp.127-134, 2008.

[27] Y. Cho, V. A. Pham Ba, J.-Y. Jeong, Y. Choi and S. Hong, "Ion-selective carbon nanotube field-effect transistors for monitoring drug effects on nicotinic acetylcholine receptor activation in live cells," *Sensors,* vol. 20, pp.3680, 2020.

[28] Shazia Rashid, Faisal Bashir, Farooq A. Khanday and M. Rafiq Beigh, "L-Shaped High Performance Schottky Barrier FET as Dielectrically Modulated Label Free Biosensor," *IEEE Transactions on Nanobioscience,* vol. 21, pp.542-548, 2022.

[29] Ashish Kumar Singh, Manas Ranjan Tripathy, Kamalaksha Baral and Satyabrata Jit, "GaSb/GaAs Type-II Heterojunction TFET on SELBOX Substrate for Dielectric Modulated Label-Free Biosensing Application", *IEEE Transactions on Electron Devices,* vol. 69, pp.5185-5192, 2022.

[30] Anju Gedam, Bibhudendra Acharya and Guru Prasad Mishra, "Design and Performance Assessment of Dielectrically Modulated Nanotube TFET Biosensor", *IEEE Sensors Journal,* vol. 21, pp.16761-16769, 2021.

[31] Synopsys Sentaurus TCAD tool, Device User Guide Version-G, 2012-06.

[32] Fabien Bibi, Maud Villain, Carole Guillaume, Brice Sorli and Nathalie Gontard, "A Review: Origins of the Dielectric Properties of Proteins and Potential Development as Bio-Sensors", *Sensors,* vol. 16, pp.1232, 2016.